Flux Line Lattice Reorientation in the Borocarbide Superconductors with $H \parallel a$

M. R. Eskildsen,[1,*] A. B. Abrahamsen,[1] D. López,[2] P. L. Gammel,[2] D. J. Bishop,[2] N. H. Andersen,[1] K. Mortensen,[1] and P. C. Canfield[3]

[1]*Risø National Laboratory, P.O. Box 49, DK-4000 Roskilde, Denmark*
[2]*Bell Laboratories, Lucent Technologies, 700 Mountain Avenue, Murray Hill, New Jersey 07974*
[3]*Ames Laboratory and Department of Physics and Astronomy, Iowa State University, Ames, Iowa 50011*
(Received 22 June 2000)

Small angle neutron scattering studies of the flux line lattice in $LuNi_2B_2C$ and $ErNi_2B_2C$ induced by a field parallel to the a axis reveal a first order flux line lattice reorientation transition. Below the transition the flux line lattice nearest neighbor direction is parallel to the b axis, and above the transition it is parallel to the c axis. This transition cannot be explained using nonlocal corrections to the London model. In addition, the anisotropy of the penetration depth λ and the coherence length ξ change at the transition.

DOI: 10.1103/PhysRevLett.86.320 PACS numbers: 74.60.Ge, 74.70.Dd

Studies of the topology of the magnetic flux line lattice (FLL) in type-II superconductors have a rich history, beginning with decoration and neutron scattering experiments on low-κ superconductors such as niobium [1]. The interplay between the symmetry in the screening current plane and nonlocal flux line interactions underpinned the menagerie of vortex lattices observed in these early experiments [2]. Interest in the vortex lattice morphology was revitalized by recent studies of the high-κ borocarbide superconductors.

The borocarbide superconductors are quaternary intermetallic superconductors with stoichiometry RNi_2B_2C ($R = Y, Dy\text{-}Tm, Lu$), organized in a tetragonal unit cell composed of alternating layers of RC and Ni_2B_2 planes [3]. They are strongly type-II superconductors with Ginzburg-Landau parameters in the range $\kappa = 6\text{–}15$. The discovery of a square FLL for $\boldsymbol{H} \parallel \boldsymbol{c}$ [4] and its transition to hexagonal symmetry at low fields [5,6] make up the first observation of a field induced FLL symmetry transition in a high-κ superconductor. Using nonlocal corrections to the London model and incorporating the symmetry of the screening currents obtained from band structure calculations, Kogan *et al.* were able to explain this transition [7]. This model was further able to predict the 45° reorientation transition of the FLL for $\boldsymbol{H} \parallel \boldsymbol{c}$ [8] and quantitatively explain systematic studies of the square to hexagonal transition in doped samples [9].

The model of Kogan *et al.* predicts a similar set of FLL transitions for fields parallel to the a axis. In this Letter we present small angle neutron scattering (SANS) studies of the FLL in this geometry. We observe a first order reorientation transition of the roughly hexagonal FLL for both magnetic and nonmagnetic borocarbide superconductors. At fields below the transition the FLL is aligned with the nearest neighbor direction parallel to the b axis. Above the transition it is parallel to the c axis. This transition is not predicted by the theory. Our data show that the anisotropy in the bc plane of both the penetration depth λ, extracted from the distortion of the FLL, and of the coherence length ξ, extracted from measurements of the angular dependence of the upper critical field, change at the reorientation transition.

The FLL was studied using the SANS spectrometer on the cold neutron beam line at the Risø National Laboratory DR3 research reactor as previously described [4–6]. The samples [3] were single crystals of $LuNi_2B_2C$ and $ErNi_2B_2C$ with T_c of 16.6 and 10.5 K, respectively. In addition $ErNi_2B_2C$ orders magnetically in an incommensurate modulated antiferromagnetic state at $T_N = 6$ K and into a weakly ferromagnetic state below $T_{WF} = 2.3$ K [10]. The magnetic field and the incoming neutrons were applied parallel to the crystalline a axis. To optimize the experiment in this geometry, the as grown crystals were cut into rods of 1 mm thickness and the pieces were individually rotated and mounted side by side forming a thin slab with the surface normal parallel to the a axis as a composite sample. Both the b and c axes of the rods were aligned using x rays to better than 3°, significantly below the SANS instrumental resolution in the scattering plane. The SANS data were taken at temperatures between 1.4 and 13 K, every time following a constant field cooling procedure from a temperature above T_c. In this scattering geometry there is increased scattering from crystal surfaces parallel to the incoming beam, necessitating subtraction of zero field cooled background measurements from the data to see the FLL diffraction patterns.

In Fig. 1 we show FLL diffraction patterns obtained at 2 K for applied fields of 2, 3.1, and 3.5 kOe in $LuNi_2B_2C$. The figure clearly shows the FLL undergoing a transition between two discrete orientations. The FLL orientations with respect to the crystallographic axes are shown in the middle panel. The relation between reciprocal and real space is given by a 90° rotation of the images, and at low fields the FLL is hence oriented with the nearest neighbor direction parallel to the crystalline b axis, and at high fields with the nearest neighbor direction parallel to the c axis. The diffraction pattern at 3.1 kOe shows clearly resolved domains of the two FLL orientations coexisting,

 0031-9007/01/86(2)/320(4)$15.00

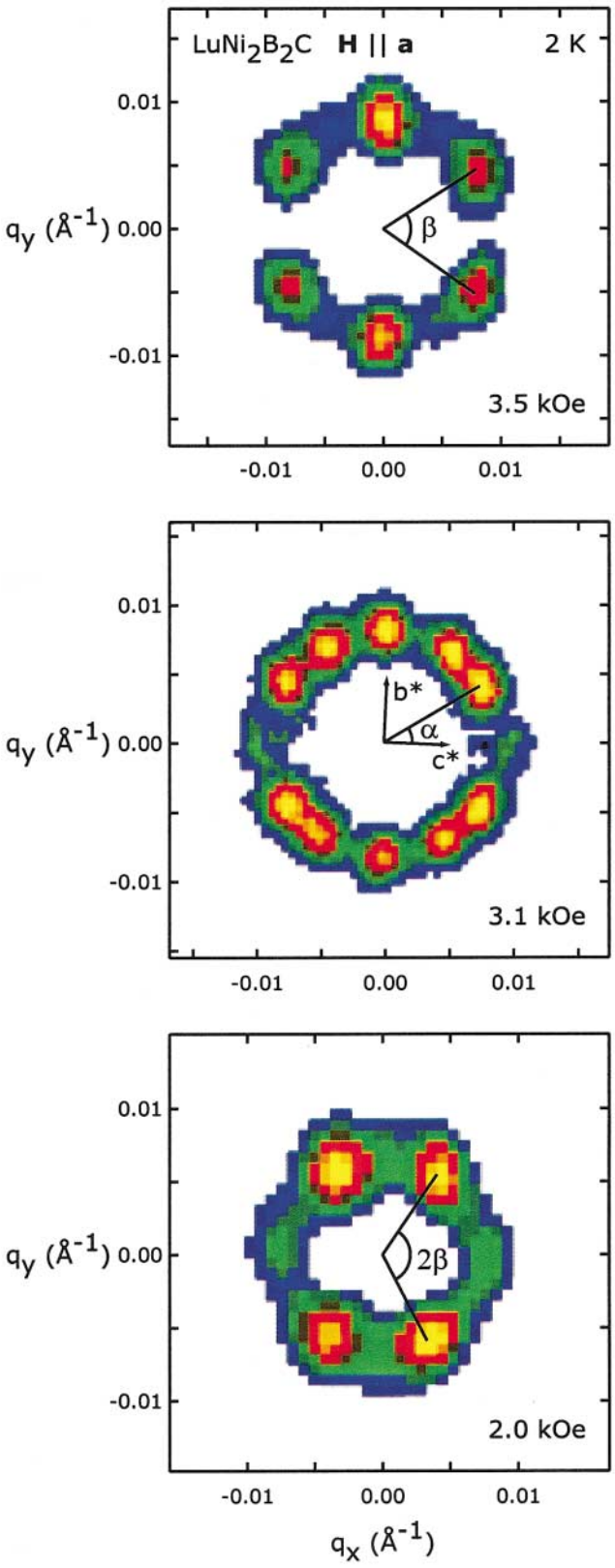

demonstrating that the reorientation does not proceed continuously, but is most probably a first order transition.

Defining the transition field, H_{tr}, at each temperature by the equal population of the two FLL orientations, we construct the phase diagram for the FLL reorientation transition shown in Fig. 2. Here the results for both $LuNi_2B_2C$ and $ErNi_2B_2C$ are plotted together with the upper critical fields. The value of H_{tr} is slightly different for the two materials, but both show only a weak temperature dependence and extrapolate to intercept H_{c2} at a nonzero field. Detailed studies at 2 K in $LuNi_2B_2C$ revealed a sharp transition, occurring in a narrow field interval of $\sim$500 Oe. Considering the FLL orientation angle α, with respect to the crystalline c axis as defined in the middle panel of Fig. 1, we observe a sharp jump at the reorientation transition shown for $LuNi_2B_2C$ in the top panel of Fig. 3. Similar results are found for $ErNi_2B_2C$, demonstrating that the FLL reorientation is unrelated to the presence or absence of magnetic ordering.

The configuration adopted by the FLL is mainly determined by the properties in the plane perpendicular to the flux lines. Field induced changes in the FLL symmetry and orientation are either driven by changes of the flux line spacing relative to the range of nonlocal flux line interactions [7], by a Fermi surface anisotropy, or by an anisotropy in the superconducting gap [11]. In the case of the square to hexagonal symmetry transition and reorientation transition for $\boldsymbol{H} \parallel \boldsymbol{c}$ the first mechanism is the driving force. However, for $\boldsymbol{H} \parallel \boldsymbol{a}$ the London model extended to include nonlocal interactions does not reproduce the reorientation transition described here [11]. Furthermore, calculations by Knigavko and Rosenstein show that the Fermi surface anisotropy in the borocarbides is insufficient to induce the FLL reorientation transition, whereas a simple gap anisotropy is capable of causing such an effect [11].

In order to further elucidate the details of the transition, we have examined two additional pieces of data. First, in Fig. 3 we show the FLL opening angle β around the crystalline c axis for both $LuNi_2B_2C$ and $ErNi_2B_2C$. This choice of β, shown in the top and bottom panels of Fig. 1, reflects the deviation of the FLL symmetry from perfectly hexagonal and allows a direct comparison between the two orientations. For both materials and orientations the FLL is

FIG. 1 (color). False color images of the FLL diffraction patterns in $LuNi_2B_2C$ at 2 K in applied fields of 3.5 kOe (top panel), 3.1 kOe (middle panel), and 2 kOe (bottom panel). The diffraction patterns are obtained following constant field cooling by summation of full rocking curves, rotating the sample around the vertical axis. The reason for the lower intensity of the reflections on the horizontal line at 2 kOe is unclear, but may be due to a variation in the ordering of the FLL along the b and c axes. The FLL orientation angle with respect to the crystalline axes α, and the opening angle β, are both determined from the position of the reflections. The shapes of the individual spots are determined by the wavelength spread of the neutron beam and its collimation given by the source and sample apertures.

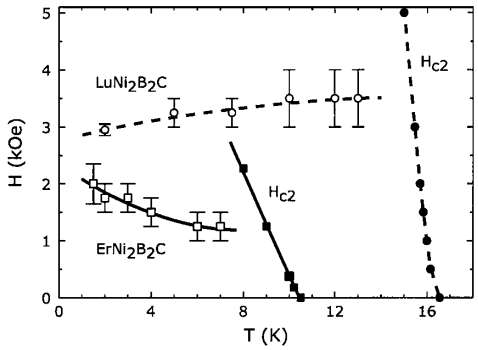

FIG. 2. Phase diagram showing the FLL reorientation transition field H_{tr}, and the upper critical field, H_{c2}, for $LuNi_2B_2C$ (circles) and $ErNi_2B_2C$ (squares). The error bars represent the precision to which H_{tr} was determined.

close to a hexagonal symmetry, with β decreasing slowly with increasing field. For $LuNi_2B_2C$ we find $\beta = 55° \pm 2°$ just below the transition, and $\beta = 62° \pm 2°$ just above. Plotting β as a function of the normalized field H/H_{tr}, all the data essentially fall on a single curve. In $ErNi_2B_2C$ β is on average smaller than in $LuNi_2B_2C$, but otherwise it follows the same general behavior. Knowing β and assuming that the FLL symmetry is distorted hexagonal, it is possible to calculate the FLL anisotropy γ, which in low field orientation is given by $\gamma = \tan(60°)/\tan\beta$ and in the high field orientation by $\gamma = \tan(30°)/\tan\beta/2$ [12]. In $LuNi_2B_2C$ γ evolves from 1 at zero field to 1.23 ± 0.03 before making the transition. At the transition γ jumps to 0.92 ± 0.02 before stabilizing at 1.04 at high fields. This corresponds to an abrupt change of the penetration depth anisotropy at the reorientation transition, which in the London model and for high-κ superconductors is given by $\gamma = \lambda_b/\lambda_c$ [13]. In $ErNi_2B_2C$ the poorer quality of the data does not allow us to determine γ just at the transition, but we can estimate $\gamma = 1.55 \pm 0.05$ and 1.1 ± 0.1, respectively, below and above H_{tr} reflecting a higher overall anisotropy in this compound. This analysis suggests that the FLL distorts gradually with increasing field $H < H_{tr}$, and that the distortion is relieved through the reorientation transition.

Second, resistivity versus temperature measurements were used to determine the angular dependence of the upper critical temperature $T_{c2}(\theta)$ when the applied field is rotated in the bc plane, which can be related directly to the coherence length variation in the screening current plane of the SANS experiment. The results of these measurements on $LuNi_2B_2C$ are summarized in Fig. 4. Qualitative similar results were observed for $ErNi_2B_2C$, although the interpretation is less clear due to the anisotropic sublattice magnetism associated with the crystal electric field splitting in this compound [14]. We show polar plots of $T_{c2}(\theta)$ at two different applied fields: $H = 1$ and 5.5 kOe. At 1 kOe (middle panel) we see a twofold modulation with a maximum in $T_{c2}(\theta)$ for $\boldsymbol{H} \parallel \boldsymbol{b}$ and a minimum for $\boldsymbol{H} \parallel \boldsymbol{c}$. Increasing the field,

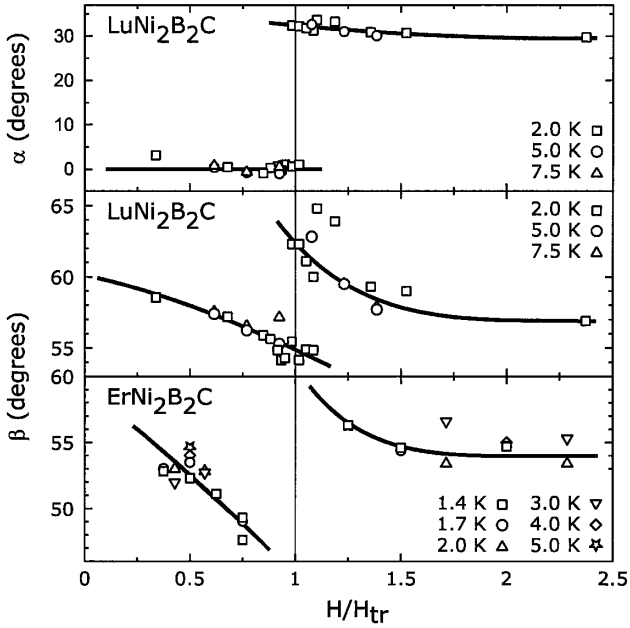

FIG. 3. Field dependence of the FLL orientation angle α for $LuNi_2B_2C$ (top panel), opening angle β for $LuNi_2B_2C$ (middle panel), and $ErNi_2B_2C$ (bottom panel). At each temperature the field axis is normalized to the transition field, H_{tr}. The measurement error is indicated by the scatter of the data points. The solid lines are guides for the eye.

the angular dependence of $T_{c2}(\theta)$ develops a secondary maximum for $\boldsymbol{H} \parallel \boldsymbol{c}$ as seen for 5.5 kOe (top panel). At this field $T_{c2}(\theta)$ still oscillates with a period of 180° but an additional fourfold component is now evident. The cusp in $T_{c2}(\theta)$ at $\boldsymbol{H} \parallel \boldsymbol{b}$ does not necessarily reflect a change of ξ, but this anomaly is in any case too small to change the results of the following analysis. Our data for $ErNi_2B_2C$ do not show this feature.

To further analyze these data we applied a Fourier transform to $T_{c2}(\theta)$ for each field to determine its modulation components. The result from this analysis for $LuNi_2B_2C$ is shown in the bottom panel of Fig. 4, where we plot the amplitude of the Fourier components of $T_{c2}(\theta)$ as a function of magnetic field. For both materials we found that this is characterized by pure *twofold* modulation at low fields (open circles). As soon as the magnetic field increases above $H \simeq 3500$ Oe (1250 Oe for $ErNi_2B_2C$), $T_{c2}(\theta)$ develops a *fourfold* modulation component (solid circles) and its twofold component starts to decrease. It is important to notice that this field coincides with the extrapolation of H_{tr} to H_{c2} suggesting a connection between the reorientation transition in the FLL and the change of the modulation of $T_{c2}(\theta)$.

The appearance of a secondary maximum in $T_{c2}(\theta)$ also produces a discontinuity in the field dependence of the ratio $T_{c2}^{\parallel b}/T_{c2}^{\parallel c}$, which we also show in the bottom panel of Fig. 4. The data show an *increasing* anisotropy at low fields changing abruptly to a *decreasing* anisotropy above $H = 4$ kOe. Furthermore, since this ratio is always greater

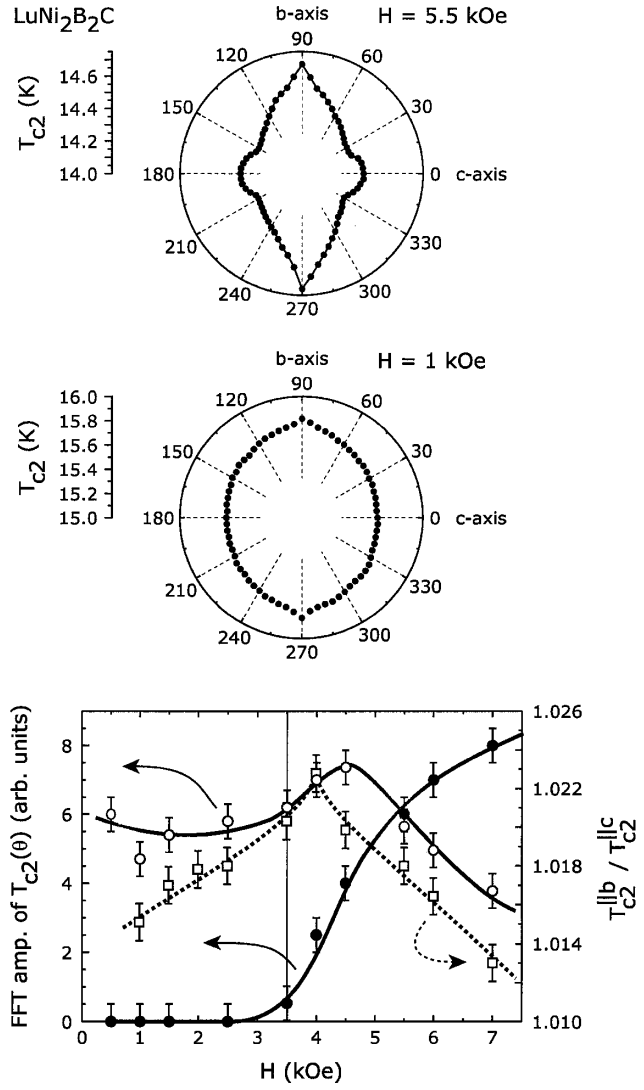

FIG. 4. Polar diagram of the angular dependence of the upper critical temperature, $T_{c2}(\theta)$ in $LuNi_2B_2C$, in applied fields of 1 kOe (middle panel) and 5.5 kOe (top panel). The magnetic field is rotated in the bc plane with $\theta = 0$ corresponding to $\boldsymbol{H} \parallel \boldsymbol{c}$. The values of T_{c2} were determined from resistivity versus temperature measurements, using a $0.9\rho_N$ criterium, where ρ_N is the normal state resistivity just above T_c. The bottom panel shows the components of the Fourier transform of $T_{c2}(\theta)$ as a function of field (left-hand ordinate). The open circles represent the amplitude for the twofold modulation component $[\cos(2\theta)]$ and the solid circles the amplitude of the fourfold modulation $[\cos(4\theta)]$. Shown in the bottom panel by the squares and using the right-hand ordinate is the ratio $T_{c2}^{\parallel b}/T_{c2}^{\parallel c}$.

than 1 we know that $H_{c2}^{\parallel b} > H_{c2}^{\parallel c}$ and hence the coherence length anisotropy $\xi_b/\xi_c > 1$. This disagrees with the usual relation $\xi_b/\xi_c = \lambda_c/\lambda_b$ if we compare with the results obtained from SANS. We have no detailed understanding of the differences in both field dependence and magnitudes of these two different measures of the anisotropy.

In summary we have used SANS to study the FLL in $LuNi_2B_2C$ and $ErNi_2B_2C$ with the applied magnetic field along the a axis. We observe a sharp reorientation transition at a field H_{tr} below which the FLL is aligned with the nearest neighbor direction parallel to the b axis, and with the nearest neighbor direction parallel to the c axis above it. For both orientations the FLL is hexagonal and slightly distorted. The sharp vortex reorientation is accompanied by changes in both the FLL anisotropy and the upper critical field bc-plane anisotropy. Theoretical work suggests that the FLL reorientation transition is driven by a superconducting gap anisotropy, but it remains unclear how this is related to the changes in the penetration depth and coherence length anisotropy at the transition.

We thank V. G. Kogan and M. E. Simon for valuable discussions. This project was supported by the Danish Technical Research Council and the Danish Energy Agency. M. R. E. was supported by the Christian and Anny Wendelbo Foundation. A. B. A. was supported by the Danish Research Academy. P. C. C. was supported by the Director of Energy Research, Office of Basic Energy Science under Contract No. W-7405-Eng.-82.

*Present address: DPMC, Université de Genève, 24 quai Ernest-Ansermet, CH-1211 Genève 4, Switzerland.
Email address: morten.eskildsen@physics.unige.ch

[1] J. Schelten, G. Lippmann, and H. Ullmaier, J. Low Temp. Phys. **14**, 213 (1974); D. K. Christen *et al.,* Phys. Rev. B **21**, 102 (1980).
[2] R. P. Huebener, *Magnetic Flux Structure in Superconductors* (Springer-Verlag, New York, 1979).
[3] For a review, see P. C. Canfield, P. L. Gammel, and D. J. Bishop, Phys. Today **51**, No. 10, 40 (1998).
[4] U. Yaron *et al.,* Nature (London) **382**, 236 (1996).
[5] M. R. Eskildsen *et al.,* Phys. Rev. Lett. **78**, 1968 (1997).
[6] M. R. Eskildsen *et al.,* Phys. Rev. Lett. **79**, 487 (1997).
[7] V. G. Kogan *et al.,* Phys. Rev. B **54**, 12 386 (1996); V. G. Kogan *et al.,* Phys. Rev. B **55**, R8693 (1997); V. G. Kogan *et al.,* Phys. Rev. Lett. **79**, 741 (1997).
[8] D. McK. Paul *et al.,* Phys. Rev. Lett. **80**, 1517 (1998); A. B. Abrahamsen *et al.,* Bull. Am. Phys. Soc. **44**, 1483 (1999).
[9] K. O. Cheon *et al.,* Phys. Rev. B **58**, 6463 (1998); P. L. Gammel *et al.,* Phys. Rev. Lett. **82**, 4082 (1999).
[10] P. C. Canfield, S. L. Bud'ko, and B. K. Cho, Physica (Amsterdam) **262C**, 249 (1996).
[11] A. Knigavko and B. Rosenstein, Phys. Rev. B **62**, 15 151 (2000).
[12] This is equivalent to fitting the position of the FLL diffraction peaks to an ellipse with the ratio γ between the major and minor axes.
[13] L. J. Campbell, M. M. Doria, and V. G. Kogan, Phys. Rev. B **38**, 2439 (1988); L. L. Daemen, L. J. Campbell, and V. G. Kogan, Phys. Rev. B **46**, 3631 (1992).
[14] B. K. Cho *et al.,* Phys. Rev. B **52**, 3684 (1995); S. L. Bud'ko and P. C. Canfield, Phys. Rev. B **61**, R14 932 (2000).